AGU PUBLICATIONS

JGR

Journal of Geophysical Research: Atmospheres

RESEARCH ARTICLE
10.1002/2015JD023657

Key Points:
- Annual mean BDC has accelerated since 1980 at 90% confidence from satellite MSU/AMSU T_{LS} observation
- Radiative component of tropical T_{LS} trend is validated using observed changes in stratospheric composition
- Relative strengthening of BDC is ~2.1%/decade, supporting the chemistry-climate model simulations

Correspondence to:
Q. Fu,
qfuatm@gmail.com

Citation:
Fu, Q., P. Lin, S. Solomon, and D. L. Hartmann (2015), Observational evidence of strengthening of the Brewer-Dobson circulation since 1980, *J. Geophys. Res. Atmos.*, *120*, 10,214–10,228, doi:10.1002/2015JD023657.

Received 11 MAY 2015
Accepted 17 SEP 2015
Accepted article online 21 SEP 2015
Published online 12 OCT 2015

Observational evidence of strengthening of the Brewer-Dobson circulation since 1980

Q. Fu[1], P. Lin[2], S. Solomon[3], and D. L. Hartmann[1]

[1]Department of Atmospheric Sciences, University of Washington, Seattle, Washington, USA, [2]Atmospheric and Oceanic Sciences Program, Princeton University, Princeton, New Jersey, USA, [3]Department of Earth, Atmospheric and Planetary Sciences, Massachusetts Institute of Technology, Cambridge, Massachusetts, USA

Abstract The change of the Brewer-Dobson circulation (BDC) over the period of 1980–2009 is examined through a combined analysis of satellite Microwave Sounding Unit (MSU/AMSU) lower stratospheric temperatures (T_{LS}), ERA-Interim reanalysis data, and observed estimates of changes in ozone, water vapor, well-mixed greenhouse gases, and stratospheric aerosols. The MSU/AMSU-observed tropical T_{LS} trend is first empirically separated into a dynamic component associated with the BDC changes and a radiative component due to the atmospheric composition changes. The derived change in the dynamic component suggests that the annual mean BDC has accelerated in the last 30 years (at the 90% confidence interval), with most of the change coming from the Southern Hemisphere. The annual mean Northern Hemisphere contribution to the acceleration is not statistically significant. The radiative component of tropical T_{LS} trends is independently checked using observed changes in stratospheric composition. It is shown that the changes in ozone, stratospheric aerosols, well-mixed greenhouse gases, and water vapor make important contributions to the radiative component of tropical T_{LS} trends. Despite large uncertainties in lower stratospheric cooling associated with uncertainties in observed ozone and water vapor changes, this derived radiative component agrees with the empirically inferred radiative component, both in terms of its average value and small seasonal dependence. By establishing a relationship between tropical residual vertical velocity at 70 hPa and T_{LS}, we show that the relative strengthening of the annual mean BDC is about 2.1% per decade for 1980–2009, supporting the results from state-of-the-art chemistry-climate model simulations.

1. Introduction

The global residual circulation of the stratosphere—the Brewer-Dobson circulation (BDC)—consists of a meridional cell in each hemisphere, with air rising across the tropical tropopause, moving poleward, and sinking into the extratropical troposphere [e.g., *Holton et al.,* 1995; *Plumb*, 2002]. General circulation models (GCMs) and chemistry-climate models (CCMs) with detailed representations of the stratosphere predict an acceleration of the BDC in response to rising greenhouse gas concentrations as well as ozone depletion [e.g., *Butchart et al.,* 2006; *Li et al.,* 2008; *Garcia and Randel*, 2008; *Oman et al.,* 2009; *Butchart et al.,* 2010; *Shepherd and McLandress*, 2011; *Lin and Fu*, 2013]. The BDC is, however, poorly constrained by observations, and many fundamental questions remain [*Butchart*, 2014]. Since the BDC and its changes have important implications on both stratospheric and tropospheric climate as well as stratospheric ozone chemistry [e.g., *Eyring et al.,* 2007; *Shepherd*, 2008; *Li et al.,* 2009; *Lamarque and Solomon*, 2010; *Birner*, 2010; *WMO*, 2011; *Fu,* 2013; *Manzini et al.,* 2014], it is important to assess the simulated BDC changes with observations.

Changes in the strength of the BDC have not been unambiguously detected from observations on the decadal time scale [*WMO*, 2011]. *Engel et al.* [2009] have analyzed balloon-borne measurements of carbon dioxide (CO_2) and sulfur hexafluoride (SF_6) over the past 30 years to derive possible trends in the mean age of stratospheric air. They reported a small but insignificant increase of the mean age of air in the Northern Hemisphere (NH) midlatitude middle stratosphere, in contrast to an expected decrease in the age of stratospheric air as a result of an accelerated BDC from GCMs and CCMs. The interpretation provided in *Engel et al.* [2009], however, has been subject to debate [*Waugh*, 2009; *Garcia et al.,* 2011]. On the other hand, observed negative ozone trends in the tropical lower stratosphere indicate increases in upwelling circulation there [*Randel and Thompson*, 2011; *Sioris et al.,* 2014].

Because of a close relationship between the variations of temperatures and residual vertical velocities in the lower stratosphere [*Yulaeva et al.,* 1994], an accelerated BDC would lead to a cooling of the tropical lower stratosphere but warming in high latitudes. Observational evidence of a long-term BDC strengthening is suggested over both the tropics and high latitudes by consistent changes in lower stratospheric temperatures [*Thompson and Solomon*, 2005; *Johanson and Fu*, 2007; *Rosenlof and Reid*, 2008; *Hu and Fu*, 2009; *Lin et al.,* 2009; *Thompson and Solomon*, 2009; *Fu et al.,* 2010; *Young et al.,* 2012]. By analyzing the lower stratospheric temperature (T_{LS}) data from satellite Microwave Sounding Unit (MSU) and advanced MSU (AMSU) for 1980–2008, *Fu et al.* [2010] found that the BDC is strengthening during June–November in the Southern Hemisphere (SH) and during December–February in the NH, but weakening during March–May in the NH. Using temperatures measured by the MSU/AMSU, Stratospheric Sounding Unit, and radiosondes, *Young et al.* [2012] confirmed a significant strengthening of the NH (SH) branch of the BDC during December (August) and a significant weakening during March in the NH. *Osso et al.* [2015] revisited the study by *Young et al.* [2012] but did not find statistically significant trends in the BDC for given months. It has still not been clear, however, whether the changes of the annual mean BDC and its NH and SH branches are statistically significant, which has important implications for the interpretation of observed changes in the mean age of stratospheric air. In addition, it remains an open question if the empirical separation of dynamic and radiative components of observed tropical T_{LS} trends can be validated using independently observed changes in atmospheric compositions. Furthermore, it is not clear how BDC changes as reflected in the tropical upwelling mass flux at 70 hPa, which is associated with the residual vertical velocity, can be related to the dynamic components of the observed T_{LS} trends. The former is a direct measure of the BDC changes, which is about 2.0–3.2% per decade from the CCMs [e.g., *Butchart*, 2014].

In this study we separate the dynamic component of the T_{LS} trends associated with the BDC changes from the radiative component following *Fu et al.* [2010]. We perform a comprehensive statistical analysis of the derived trends based on a Monte Carlo technique. We show that the strengthenings of annual mean BDC and its annual mean SH branch are statistically significant at the 90% confidence interval in the last 30 years, while the strengthening of the annual mean NH BDC is smaller and statistically insignificant. The latter implies an insignificant long-term change of the mean age of stratospheric air in the NH. We also independently estimate tropical radiative cooling based on observed changes in ozone, water vapor, well-mixed greenhouse gases, and stratospheric aerosols, which is complementary to the empirically derived radiative cooling. The latter is obtained as the difference between the observed tropical T_{LS} trend and its dynamical component. The comparison of the radiative contributions from these two independent methods by month supports the notion that the seasonality of observed tropical T_{LS} trends in the last 30 years is largely a response to changes in the BDC [*Fu et al.,* 2010]. We further probe the relationship between tropical mean residual vertical velocity at 70 hPa and T_{LS} so that the dynamic component of tropical T_{LS} trends can be related to the change of residual vertical velocity. We find that the BDC in the last 30 years has strengthened by ~2.1% per decade in terms of tropical mean residual vertical velocity at 70 hPa.

This paper is organized as follows. Section 2 describes the suite of data employed. The trend in lower stratospheric temperature (T_{LS}) and its dynamic and radiative components are discussed in section 3, and the statistical analysis of the derived trends is given in section 4. The tropical radiative cooling estimated from observed changes in stratospheric composition is presented in section 5. The long-term change of the BDC in terms of tropical vertical velocity based on lower stratospheric temperature trends is then examined in section 6. The summary and conclusions are given in section 7.

2. Data

We used the MSU/AMSU lower stratospheric temperature (T_{LS}) monthly anomalies, in which the mean seasonal cycle for 1980–2009 is removed. They are gridded at 2.5° latitude by 2.5° longitude. The T_{LS} weighting function ranges from ~20 hPa to ~120 hPa and peaks around 60–70 hPa [e.g., *Fu and Johanson*, 2005], which therefore represents well the lower stratosphere. The T_{LS} channel has some contribution from the tropical upper troposphere, and we estimate its impact in section 4. The MSU/AMSU measurements extend to 82.5°N/S. In this study, we define the tropics from 20°S to 20°N and high latitudes from 40°N(S) to 82.5°N(S) following *Fu et al.* [2010]. *Lin et al.* [2009] and *Fu et al.* [2010] showed that outside the tropics the strongest signal of T_{LS} changes associated with the BDC is around 65°N/S. Note that our analysis does not require a complementary division of latitudes, although we obtain similar results by defining the tropics from 30°S to 30°N and high latitudes

from 30°N(S) to 82.5°N(S) (not shown). Three T_{LS} data sets are available, which are compiled by the University of Alabama at Huntsville team [*Christy et al.,* 2003, hereinafter UAH], the Remote Sensing System team [*Mears and Wentz,* 2009, hereinafter RSS], and the National Oceanic and Atmospheric Administration team [*Zou et al.,* 2006, hereinafter NOAA]. Note that the NOAA team employed a unique inter-satellite calibration algorithm for the MSU/AMSU instruments using simultaneous nadir overpasses. In this study, we used T_{LS} from all three data sets but present the results obtained with the NOAA data set unless specified.

The eddy heat flux, representing the upward-propagating wave activity, has been used as an index for the BDC, which has been empirically tested in many previous studies [e.g., *Newman et al.,* 2001]. Here the 6-hourly ERA-Interim reanalysis data [*Dee et al.,* 2011] were used to calculate the eddy heat flux, which is averaged over 3 months including the given month and two previous months, as an index of the strength of the BDC for a given month [*Lin et al.,* 2009; *Fu et al.,* 2010]. The starting year in this study is 1980 to avoid the use of reanalysis data prior to the satellite era. We also used the ERA-Interim reanalysis data to establish the relations between residual vertical velocities at 70 hPa and T_{LS} over the tropics. *Seviour et al.* [2012] found that the BDC is well represented by this reanalysis data in terms of its climatology and variability.

We also use a radiative transfer model to directly estimate tropical T_{LS} trends that are radiatively driven by the changes in stratospheric composition except aerosols (see section 5). We impose the tropical monthly mean temperature, ozone, and water vapor profiles compiled by *Yang et al.* [2008] as background atmospheric profiles against which perturbations are applied. This background climatology is based on several data sources. The temperature and ozone profiles at least up to 28 km were obtained from 14 Southern Hemisphere Additional Ozonesonde [*Thompson et al.,* 2003] stations. The water vapor profiles, measured by the cryogenic frost-point hygrometer as well as the NOAA/CMDL (now NOAA/ESRL) frost-point hygrometer balloon soundings, were obtained from seven tropical stations. In order to obtain accurate radiative heating rate calculations in the tropical lower stratosphere, the observed atmospheric profiles are extended up to 0.2 hPa by blending in the United Kingdom Meteorological Office monthly stratospheric analysis of temperature data and Halogen Occultation Experiment (HALOE) monthly ozone and water vapor data. We did radiative transfer calculations using different background profiles, which has little effect on our results.

Observed monthly ozone trend profiles came from three different data sets [see, e.g., discussion of tropical ozone in *Solomon et al.,* 2012]: *Randel and Wu* [2007, hereinafter RW], *Cionni et al.* [2011, hereinafter SPARC], and *Hassler et al.* [2009, hereinafter BDBP]. Time-dependent surface concentrations of well-mixed greenhouse gases including CO_2, methane (CH_4), nitrous oxide (N_2O), and chlorofluorocarbons (CFCs) observed at the Mauna Loa station were from the NOAA/ESRL Global Monitoring Division archive, which were imposed for the entire column of the atmosphere. Observed monthly mean stratospheric aerosol optical depths at 0.55 μm were taken from *Sato et al.* [1993] for the period before 1998 and from *Vernier et al.* [2011] afterwards to consider the stratospheric aerosol effects [*Solomon et al.,* 2011].

High-quality global satellite observations of stratospheric H_2O began in the 1990s, and information on stratospheric H_2O trends was also available from balloon observations at a single site in Boulder, Colorado, beginning in 1980 [*Oltmans et al.,* 2000]. From these data, a sharp drop in stratospheric H_2O was documented after the year 2000 [*Randel et al.,* 2006], and the lower levels have persisted up to the mid-2009 [*Solomon et al.,* 2010]; another sharp drop occurred in 2013 [*Dessler et al.,* 2013]. Before the first decrease, the balloon data suggest a gradual midlatitude increase in lower stratospheric H_2O of more than 1 ppmv from 1980 to 2000 and the satellite observations also support increases in lower stratospheric H_2O during the 1990s. Following *Solomon et al.* [2010], the effects of water vapor changes were estimated by considering two H_2O change scenarios. In the first of these (hereinafter H_2O-I), the H_2O change only occurred between January 2000 and June 2001 and there are no H_2O changes before and after this period. The altitude and latitude distribution of the H_2O changes in the stratosphere after 2000 was derived from the HALOE data [*Russell et al.,* 1993] as the monthly differences between the average from June 2001 to May 2005 and that from January 1996 through December 1999. In a second scenario (hereinafter H_2O-II), it was assumed that H_2O had increased uniformly by 1 ppmv at all latitudes and altitudes above 14 km between January 1980 and December 1999 and then followed the changes in H_2O-I. The water vapor change is set to be zero at and below 14 km. Since the data before the mid-1990s are limited in space and/or time, the stratospheric H_2O trends before 2000 should be considered to be uncertain, whereas the decrease after 2000 is much better characterized by multiple sensors [*Solomon et al.,* 2010].

The lower tail of the T_{LS} weighting function can reach as low as 200 hPa [e.g., *Fu and Johanson*, 2005], and the T_{LS} trends might thus be affected by the tropical upper tropospheric warming [*Fueglistaler et al.,* 2011]. We used tropical tropospheric temperature trend profiles from the Geophysical Fluid Dynamic Laboratory (GFDL) global High Resolution Atmospheric Model (HiRAM) at ~50 km horizontal grid size (C180) [*Zhao et al.,* 2009] to estimate the impact of tropospheric changes on T_{LS}. The simulations from GFDL-HiRAM-C180 forced by observed sea surface temperatures (SSTs) and sea ice concentrations (SICs) for 1979–2008 are available from Phase 5 of the Coupled Model Intercomparison Project archive [*Taylor et al.,* 2012]. *Po-Chedley and Fu* [2012] showed that the ratio of tropical upper tropospheric warming to lower middle tropospheric warming from this model agrees well with satellite MSU/AMSU observations. We used the simulations from GFDL-HiRAM-C180 for 1979–2008.

To compare our observational estimates with the model-simulated BDC acceleration, we used the model output from 11 CCMs participating in the Chemistry-Climate Model Validation activity phase 2 (CCMVal-2) [*SPARC CCMVal*, 2010]. These are state-of-the-art CCMs that are employed to predict ozone recovery in the recent ozone assessment [*WMO*, 2011]. Detailed representations of stratospheric dynamical, radiative, and chemical processes are included in these models but vary much from model to model. We analyzed simulations from the REF-B1 scenario for 1980–2004, in which all forcings and SSTs/SICs were taken from the observations. See *Lin and Fu* [2013] for more details on the CCM data and analyses.

3. Changes in Lower Stratospheric Temperatures

An approximate linearized form of the transformed Eulerian mean thermodynamic energy equation [*Andrews et al.,* 1987; *Yulaeva et al.,* 1994; *Randel et al.,* 2002; *Fueglistaler et al.,* 2011] can be written as

$$\partial\overline{T}/\partial t = \overline{Q} - \overline{w}^{*}S, \tag{1}$$

where $\overline{T}$, $\overline{Q}$, and $\overline{w}^{*}$ are the zonal mean temperature, radiative heating, and residual vertical velocity, respectively, and S is a stability parameter. The radiative heating is often approximated by the Newtonian cooling in a form $\overline{Q} = -k_{rad}\left(\overline{T} - \overline{T}_{E}\right)$ where $\overline{T}_{E}$ is a radiative equilibrium temperature and $1/k_{rad}$ is the radiative damping time that is in the order of 30–90 days in the lower stratosphere [e.g., *Randel et al.,* 2002; *Fueglistaler et al.,* 2009]. When considering the long-term trends of equation (1), the trend in temperature tendency is negligible (i.e., $\partial\overline{T}/\partial t \approx 0$) so that the trend in diabatic heating is approximately balanced by the upwelling-induced adiabatic cooling. Therefore, we have

$$k_{rad}\left(\overline{T} - \overline{T}_{E}\right) \approx -\overline{w}^{*}S \tag{2}$$

Thus, the changes of zonal mean lower stratospheric temperatures are mainly related to the changes in dynamically forced upwelling $\overline{w}^{*}$ and changes in radiative equilibrium temperature $\overline{T}_{E}$. The latter is determined by the atmospheric composition. The overbar can be considered as the area mean over the tropics and the high latitudes as defined in section 2.

While CO_2 increases and O_3 chemical depletion lead to radiative cooling throughout the stratosphere, an accelerating BDC leads to a dynamic cooling in the tropical lower stratosphere where air is rising, and warming in high-latitudes where air is sinking [see equation (2)]. We separated observed high-latitude T_{LS} trends into a dynamic component due to the change of the BDC and a radiative component following *Fu et al.* [2010]. A brief description of the method is given here; see *Fu et al.* [2010] for more details.

To represent the strength of the BDC responsible for T_{LS} changes for a given month, the 3-month (i.e., the month considered and two previous months) mean eddy heat flux averaged over the high latitudes of each hemisphere (40°S–90°S/40°N–90°N) and vertically averaged between 10 and 50 hPa was used. The time lag between T_{LS} and wave activities largely comes from the radiative relaxation time [*Newman et al.,* 2001]. A regression of gridded T_{LS} data was performed upon the corresponding eddy heat flux index time series for each month and over each hemisphere. The attribution of the T_{LS} trend to changes in the BDC was derived by multiplying the regression maps with the linear trend in the eddy heat flux index. The T_{LS} trends due to the BDC changes were averaged over high latitudes in each hemisphere for each month. The empirically derived radiative component, averaged over 40–82.5°S(N), is termed the observed total T_{LS} trend minus the dynamic component, averaged over the same region. Note that although changes of polar planetary waves in terms of

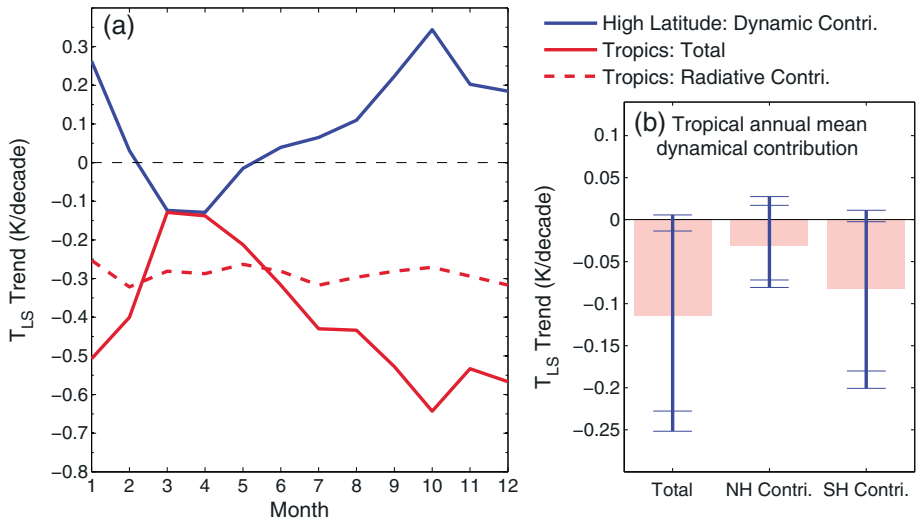

Figure 1. MSU/AMSU lower stratospheric temperature (T_{LS}) trends for 1980–2009 (K/decade). (a) The T_{LS} trends due to the change of the Brewer-Dobson circulation (BDC) over combined high latitudes (40°N–82.5°N and 40°S–82.5°S) (blue solid line) and observed T_{LS} trends in the tropics (20°N–20°S) (red solid line) along with its estimated radiative component (red dashed line), versus month. (b) The annual mean T_{LS} trend due to the change of the BDC in tropics and its contribution from the Northern Hemisphere (NH) and Southern Hemisphere (SH) cells. The blue lines in Figure 1b indicate the 90% and 95% confidence intervals of the derived trends.

magnitude and/or phase may affect the spatial pattern of the T_{LS} trend [*Lin et al.,* 2009], these have little direct impact on the trend averaged over the NH/SH high latitudes.

The blue solid line in Figure 1a shows the T_{LS} trends due to BDC changes obtained in this manner, averaged over high latitudes of the two hemispheres combined (i.e., over 40–82.5°S and 40–82.5°N) as a function of month. The observed T_{LS} trends over the tropics are also shown in Figure 1a (red solid line) for a direct comparison. We see a near-perfect negative correlation between observed tropical T_{LS} trends and the high latitude T_{LS} dynamic components, suggesting that the monthly dependence of observed tropical T_{LS} trend is largely caused by the BDC changes [*Fu et al.,* 2010]. The observed T_{LS} trends in the tropics (solid red line) can be separated into two parts as follows:

$$T_{\mathrm{LS,Tropics}} = aT_{\mathrm{LS,\ High\text{-}Lat,\ Dyn}} + \left(T_{\mathrm{LS,Tropics}} - aT_{\mathrm{LS,\ High\text{-}Lat,\ Dyn}}\right), \tag{3}$$

where a is a coefficient obtained from orthogonal least squares fitting between the red ($T_{\mathrm{LS,Tropics}}$) and blue ($T_{\mathrm{LS,\ High\text{-}Lat,\ Dyn}}$) solid lines across all months (which displays a correlation of 0.96). The observed T_{LS} trends in the tropics are thus separated into the BDC change-induced dynamic component [the first term on the right hand side of equation (3)] and a residual [the second term on the right hand side of equation (3); also see dashed red line in Figure 1a]. The latter obtained as the difference between the observed tropical T_{LS} trend and the dynamical component is here called the empirically derived radiative component of tropical T_{LS} trends. Note that in the above approach, the radiative component of month-to-month variability that is correlated with the BDC changes will become part of the dynamic component. We will discuss this in section 5 in more detail, when we compare the empirically derived radiative component with that directly derived from the changes of atmospheric compositions.

The observed annual mean T_{LS} trends in the tropics are −0.40, −0.34, and −0.4 K/decade for 1980–2009 from UAH, RSS, and NOAA data sets, respectively (Table 1). The corresponding empirically derived radiative components using these data sets have annual mean trends of −0.29, −0.23, and −0.29 K/decade, all showing small seasonal dependencies. The derived annual mean dynamic contribution is −0.11 K/decade, which is independent of the MSU/AMSU data used. Note that we obtain a similar dynamic contribution (−0.1 K/decade) by considering the tropics from 30°S to 30°N and high latitudes from 30°N(S) to 82.5°N(S).

Critical support for the above results is provided by the fact that the monthly dependencies and annual mean values of these empirically derived radiative components are consistent with radiatively driven trends

Table 1. Annual Mean T_{LS} Trends (K/decade) Observed From Satellite MSU/AMSU for 1980–2009 and Empirically Derived Dynamic and Radiative Contributions (Section 3)

	UAH	RSS	NOAA
Total	−0.40	−0.34	−0.40
Dynamic contribution	−0.11	−0.11	−0.11
Radiative contribution	−0.29	−0.23	−0.29

estimated using observed changes in stratospheric composition associated with O_3, H_2O, well-mixed greenhouse gases, and stratospheric aerosols (see section 5). Furthermore, the derived dynamic component of T_{LS} here is consistent with that in *Fu et al.* [2010], where the NCEP/NCAR reanalysis data were used. By using the ERA-Interim reanalysis, however, the adjustments in *Fu et al.* [2010] are not needed and the derived dynamic contributions are insensitive to the MSU/AMSU data sets used (not shown).

This study indicates that the ERA-Interim eddy heat flux trend, which is used as a measure of the BDC changes, is reliable and robust. Compared to the reanalyses, we have more confidence on the MSU/AMSU data in terms of the long-term trends and this is why we employed the MSU/AMSU T_{LS} as the main variable. Our analysis combining the MSU/AMSU T_{LS} and reanalysis eddy heat flux, as well as the consistency check of the T_{LS} trend spatial pattern, monthly dependence, and its radiative and dynamic components, support our confidence in the reanalysis eddy heat flux trend [*Lin et al.,* 2009; *Fu et al.,* 2010]. The radiative component of T_{LS} trend derived from an independent approach (section 5) further validates the use of the reanalysis eddy heat flux trend. Note that the validity of the reanalysis eddy heat flux trend does not, however, guarantee the validity of the reanalysis w^* trend [*Seviour et al.,* 2012].

4. Confidence Interval of Derived T_{LS} Trends

The confidence intervals in the derived trends are determined using a Monte Carlo method. By using the symbol X to denote MSU T_{LS} or eddy heat flux index, the time series of X for a given month, i, can be separated into a linear trend part X_L and its deviation from the trend, X_D, i.e.,

$$X(i,\text{year}) = X_L(i,\text{year}) + X_D(i,\text{year}) \tag{4}$$

where $i = 1, \ldots, 12$ and year = 1980, …, 2009. X_L can be written in the form

$$X_L(i,\text{year}) = K(i)^*(\text{year} - \text{year}_{\text{mid}}) + A(i) \tag{5}$$

where $K(i)$ is the trend of X for a given month i, as determined from the least-square fitting, year_{mid} is 1994.5, and $A(i)$ is the mean of X for the given month. A synthetic time series X' is then created for each month by randomly switching the order of year for X_D while keeping X_L unchanged, viz., $X' = X_L + X_D'$. We create such synthetic time series for T_{LS} over the tropics and high latitudes as well as for the eddy heat flux index. Note that the switched order is the same for T_{LS} and the eddy heat flux index. We then derive the total, dynamical, and radiative components of the T_{LS} trends in each synthetic set of time series as in the original one. The probability distribution function for any selected variable is calculated from results of 10,000 synthetic sets.

The BDC change-induced T_{LS} annual mean trend and the contributions from the NH and SH cells are shown in Figure 1b for the tropics. The tropical NH and SH contributions to the BDC trends were computed by multiplying the corresponding high latitude NH and SH dynamical contributions by the coefficient a in equation (3). Both 90% and 95% confidence intervals of these trends are shown. We obtain a dynamic cooling in tropical T_{LS} that is significant at the 90% confidence interval, indicating a strengthening of the BDC in the past three decades. Figure 1b also shows that the annual mean strengthening of the BDC SH (NH) cell is statistically significant (insignificant) at a 90% confidence interval. This result is consistent with that of *Garcia and Randel* [2008], obtained from numerical simulations. The dynamic cooling in tropical T_{LS} is mainly a result of the BDC strengthening in the SH cell (about three fourths), and a contribution to the BDC strengthening from the NH cell is small (about one fourth) (Figure 1b).

Figure 2 presents the probability density function of the annual mean dynamic component of tropical T_{LS} trend, with dark and light shading showing the 90% and 95% confidence intervals, respectively. The probability of a positive value (i.e., a deceleration of the BDC rather than acceleration) is only about 2.5%. Note that the probability density function shown in Figure 2 is not a normal distribution.

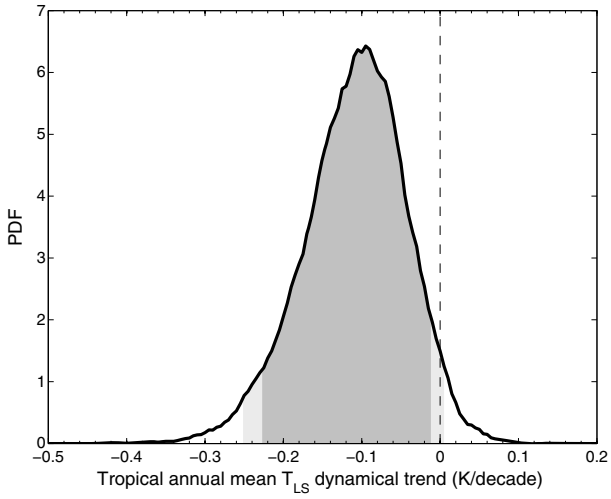

Figure 2. Probability density function of the dynamic component of tropical T_{LS} trends as a result of the BDC changes for 1980–2009 based on a Monte Carlo technique.

Figure 3 shows monthly T_{LS} total trends (left), and their dynamic (middle) and radiative (right) contributions for SH high latitudes (upper), NH high latitudes (middle-upper), combined high latitudes (middle-lower), and tropics (lower), along with their 90% (red shade) and 95% (blue shade) confidence intervals. The radiative contribution is obtained as the residual of the total minus the dynamic contribution. The annual mean trend values and their 90% and 95% confidence intervals are shown on the right in each chart using red solid circles and red and blue lines. We obtain a statistically significant BDC strengthening at the 95% confidence interval for the SH cell in October (Figure 3b), for the NH cell in January (Figure 3e), and for the total BDC in October and November (Figure 3h or Figure 3k). At the 90% confidence interval, the BDC strengthening is statistically significant for the SH cell from September to November (Figure 3b), for the NH cell in December and January (Figure 3e), and for the total BDC from September to January (Figure 3h or Figure 3k). Almost

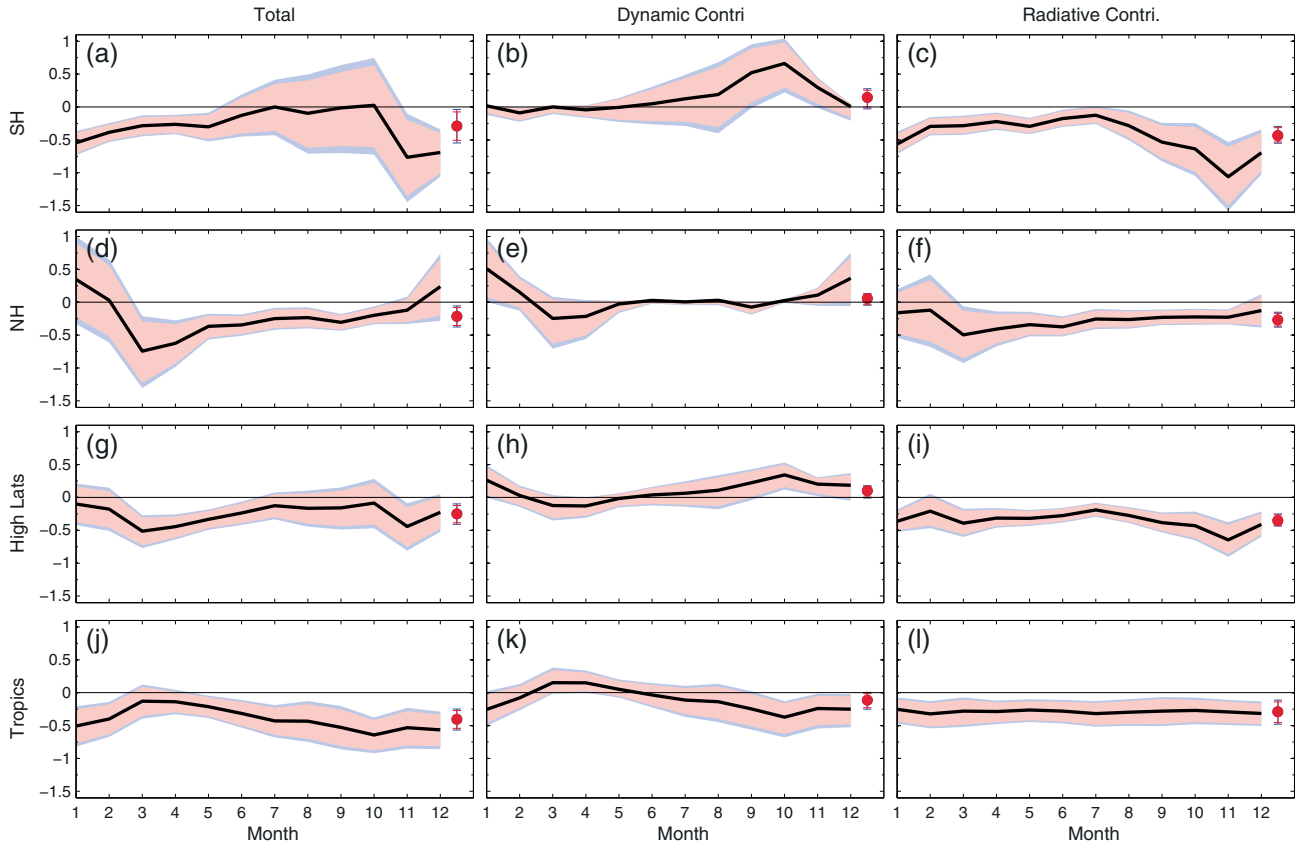

Figure 3. MSU/AMSU lower stratospheric temperature (T_{LS}) trends for 1980–2009 (K/decade) versus month for (left) observed total, (middle) BDC-induced dynamic contributions, and (right) radiative contributions over (upper) SH high latitudes (40°S–82.5°S), (middle-upper) NH high latitudes (40°N–82.5°N), (middle-lower) combined high latitudes (40°N–82.5°N and 40°S–82.5°S), and (lower) tropics (20°N–20°S). The red and blue shades indicate the 90% and 95% confidence intervals of the derived trends, respectively. The annual mean values of these trends are shown in solid red circles with the 90% and 95% confidence intervals indicated by the red and blue lines, respectively.

all radiative contributions are statistically significant except over NH high latitudes from December to February (Figure 3f).

Osso et al. [2015] examined the BDC trends by analyzing the MSU/AMSU T_{LS} data. Following *Young et al.* [2012], they defined a BDC index as BDCI_T = T_extr − T_trop for each month, where T_extr and T_trop are the extratropical and tropical mean T_{LS} monthly anomalies, respectively. *Osso et al.* [2015] did not find a statistically significant BDC trend at the 95% confidence interval for October and November as we did (compare their Figure 5 right lower panel with our Figure 3k). By using the BDCI_T as the BDC index in *Osso et al.* [2015], it is assumed that the extratropical radiative component cancels the tropical one. In contrast, we find that the radiative cooling in the extratropics is often larger than that in the tropics (Figures 3i and 3l); this is particularly true in October and November, for example, leading to an underestimation of the BDC trends if radiative terms are assumed to cancel each other out.

Engel et al. [2009] suggested that no annually averaged acceleration has occurred in the BDC over the past 30 years, based upon an unchanged mean age of air in the NH middle stratosphere estimated from balloon observations of SF_6 and CO_2 concentrations. Our results suggest that the strengthening of the total BDC need not be inconsistent with an unchanged mean age of air in the NH midlatitude stratosphere, since only a small, statistically insignificant annual mean change is obtained in the BDC NH cell (Figure 1b). This small annual mean change arises in part because the weakening of the BDC in the NH cell in March and April partly cancels a strengthening in December–February [*Fu et al.,* 2010; *Free*, 2011] (Figure 3e). Note that although most data used by *Engel et al.* [2009] were available between May and October, the change in mean age of the stratospheric air should largely depend on the annual mean BDC changes since it takes about 4–5 years for an air parcel to reach there from the tropical tropopause.

5. Radiative Contribution to Tropical T_{LS} Trends

The empirically derived radiative contribution in tropical T_{LS} trends (red dashed line in Figure 1a) has a small seasonal dependence, with annual mean values of −0.23 to −0.29 K/decade depending on the MSU/AMSU data sets used (Table 1). Here we compare this quantity to estimates based on observed changes in well-mixed greenhouse gas concentrations (CO_2, CH_4, N_2O, and CFCs), O_3, and H_2O (section 5.1) and stratospheric aerosols (section 5.2). We also consider the impact of tropical upper tropospheric warming on T_{LS} (section 5.3).

5.1. Well-Mixed Greenhouse Gases (CO_2, CH_4, N_2O, and CFCs), O_3, and H_2O

The impact of the changes in well-mixed greenhouse gases, O_3, and H_2O on tropical T_{LS} trends is calculated with the NASA Langley Fu-Liou radiation model [*Fu and Liou*, 1992; *Rose and Charlock*, 2002] and the Rapid Radiative Transfer Model [*Mlawer et al.,* 1997; *Mlawer and Clough*, 1998]. Since the results using the two models are very similar, we show here only those from the Fu-Liou radiation model. We estimate the changes in T_{LS} using the "Seasonally Evolving Fixed Dynamical Heating" method [*Forster and Shine*, 1997; *Fueglistaler et al.,* 2011] where the dynamical heating does not change when the composition is perturbed. A monthly climatological dynamical heating at each level from the tropical tropopause to 60 km is calculated from the temperature tendency of the annual cycle minus the radiative heating, which is then fixed when trace gases are perturbed, leading to the changes in stratospheric temperatures. We do not assume Newtonian cooling in this framework. Note that the "Fixed Dynamic Heating" method [*Forster and Shine*, 1997], which does not consider the temperature annual cycle tendency, yields the same annual mean values of temperature changes but does not produce an accurate monthly dependence. The calculated stratospheric temperature profile for each month is converted to T_{LS} using the T_{LS} weighting function.

The tropical T_{LS} trends that are radiatively driven as a result of changes in well-mixed greenhouse gases, O_3, and H_2O are shown in Figure 4a. The tropical T_{LS} trends due to changes in well-mixed greenhouse gases show little monthly dependence (green solid line), with an annual mean value of −0.09 K/decade. More than 90% of this trend is caused by the CO_2 increase (not shown). The radiative trends caused by O_3 changes shown in Figure 4a (red solid line) are based on the RW O_3 data set. They show some monthly dependence, with a phase delayed by about 2 months relative to that in observed T_{LS} total trends (comparing the red solid line in Figure 4a with the red solid line in Figure 1a). This is because the ozone change is dominated at this altitude not by chemical depletion but rather by the change of ozone transport associated with the BDC change

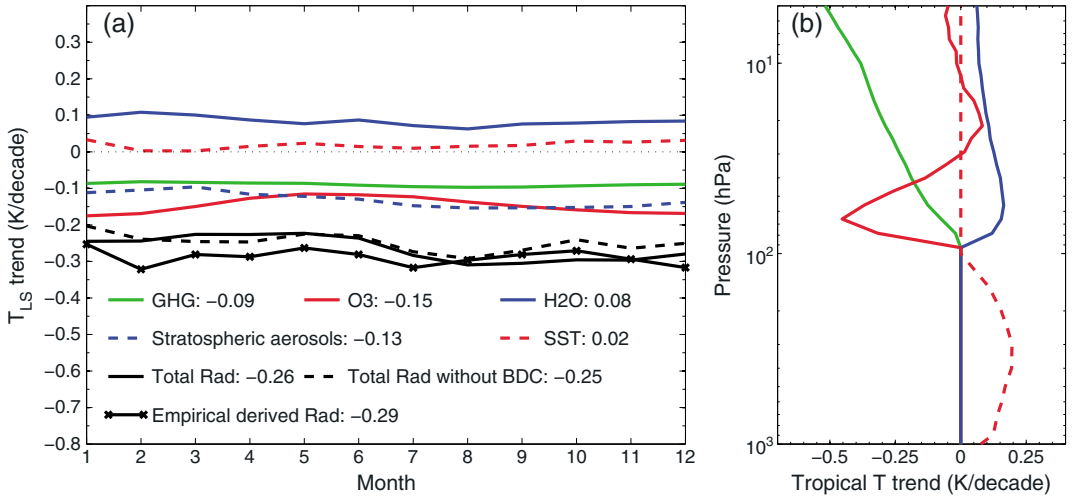

Figure 4. (a) Radiative contributions to T_{LS} trends (K/decade) for 1980–2009 in tropics (20°N–20°S) due to the changes of well-mixed greenhouse gases (green solid line), O_3 (red solid line), H_2O (blue solid line), stratospheric aerosols (blue dashed line), tropical upper tropospheric warming associated with sea surface temperatures (SSTs) (red dashed line), and the summation of these contributions (black solid line). The total radiative contribution after removing the part that is correlated with the BDC change is shown as the black dashed line. The empirically derived radiative component from Figure 1a is also shown (black solid line with x symbol) for comparison. (b) The annual mean tropical temperature trend profiles that are used to derive the corresponding annual mean T_{LS} trend values shown in Figure 4a.

[*Lamarque and Solomon*, 2010], and the radiative relaxation time in the lower stratosphere is about 30 to 90 days [*Randel et al.,* 2002]. The annual mean value of radiative trends caused by the RW O_3 changes is −0.15 K/decade. A similar monthly dependence of these radiative trends is obtained using the SPARC O_3 data set but with a slightly smaller annual mean value of −0.12 K/decade. The annual mean radiative trend from the BDBP O_3 data set is −0.4 K/decade, which is about three times larger than the RW and SPARC values [*Solomon et al.,* 2012].

The radiative effect of water vapor using H_2O-I is shown in Figure 4a (blue solid line); this term has a small seasonal dependence with a mean value of 0.08 K/decade. The annual mean radiative trend using H_2O-II is −0.07 K/decade, which has a similar absolute value to H_2O-I but an opposite sign. Because of large uncertainties in long-term changes of stratospheric water vapor before 2000 [*Fueglistaler and Haynes*, 2005], we place more confidence in the H_2O-I radiative effects.

5.2. Stratospheric Aerosol Effect

Stratospheric aerosols due mainly to volcanic eruptions of El Chichon in March 1982 and Pinatubo in June 1991 warmed the lower stratosphere. The warming lasted for about 2 years after these eruptions. Since both eruptions occurred in the first half of the period from 1980 to 2009, such warming would contribute to a cooling trend in the period considered. To quantify this effect, a regression of the tropical T_{LS} time series was performed upon the tropical stratospheric aerosol optical depth time series, and the trends of resulting T_{LS} time series were derived (i.e., the regression coefficient times the optical depth time series). The results are shown in Figure 4a (blue dashed line), which have an annual mean value of −0.13 K/decade.

We also estimate the stratospheric aerosol effect on the T_{LS} trends for 1980–2009 as the difference between the T_{LS} trends with and without considering the Pinatubo and El Chichon periods (i.e., 2 years after the eruptions including the eruption months). We obtain an annual mean value of −0.13 K/decade from the NOAA T_{LS} data, and −0.12 K/decade from the RSS and UAH data, which agrees with the result from the regression method.

5.3. SST Effect

The increase of tropical SSTs in the last 30 years would lead to an increase of tropical upper tropospheric temperatures [*Fu et al.,* 2004; *Fu and Johanson*, 2005; *Fu et al.,* 2011]. Since the weighting function of tropical T_{LS} extends to the upper troposphere, the tropical upper troposphere would have a warming effect on T_{LS}. We estimated this effect by applying the T_{LS} weighting function to tropical tropospheric warming profiles derived

Table 2. Annual Mean Radiative Contributions (K/decade) to T_{LS} Trends for 1980–2009, Calculated Based on the Changes in Stratospheric Composition Including Well-Mixed Greenhouse Gases (CO_2, CH_4, N_2O, and CFCs), O_3, and H_2O Using the Fu-Liou Radiation Scheme With the "Seasonally Evolving Fixed Dynamical Heating" Method, and the Change in Stratospheric Aerosols From a Regression Method (Section 4)[a]

Cases with Various O_3 and H_2O Data Sets	Radiative Contributions to T_{LS} Trends
Reference	−0.26
Reference but SPARC O_3	−0.24
Reference but BDBP O_3	−0.52
Reference but H_2O-II and RW O_3	−0.42
Reference but H_2O-II and SPARC O_3	−0.40
Reference but H_2O-II and BDBP O_3	−0.68

[a]The effect of tropical upper tropospheric warming on T_{LS} was also included. Three ozone data sets of RW, SPARC, and BDBP and two water vapor scenarios of H_2O-I and H_2O-II were used (section 2). The "Reference" is for the radiative contribution when the RW O_3 and H_2O-I were used.

from the GFDL-HiRAM-C180 simulations. The effect is small, with an annual mean value of 0.02 K/decade (see red dashed line in Figure 4a). This effect would introduce a bias into our empirically derived "radiative" contribution since it will appear as a residual that is not associated with the BDC changes.

The total radiative trend in T_{LS}, which is the summation of contributions from well-mixed greenhouse gases, O_3 (RW), H_2O (H_2O-I), stratospheric aerosols, and tropical upper tropospheric warming, is shown in Figure 4a (black solid line). We see a small seasonal dependence with an annual mean value of −0.26 K/decade. The case shown in Figure 4a is called the "Reference" for simplicity of presentation. Table 2 shows the total radiative trends in T_{LS} based on various O_3 and H_2O data sets along with the contributions from well-mixed greenhouse gases, stratospheric aerosols, and SSTs. It ranges from −0.24 K/decade ("Reference but SPARC O_3") to −0.68 K/decade ("Reference but H_2O_II and BDBP O_3"). We might however place more confidence in radiative trends in T_{LS} from "Reference" (−0.26 K/decade) and "Reference but SPARC O_3" (−0.24 K/decade). This is because the radiative trends using BDBP O_3 (see "Reference but BDBP O_3" and "Reference but H2O_II and BDBP O_3" in Table 2) are significantly larger than the observed total T_{LS} trends (Table 1), and there is a large uncertainty in H_2O_II as discussed above. Therefore, despite large uncertainties in lower stratospheric cooling associated with uncertainties in observed O_3 and H_2O changes there, the radiative component estimate from observed composition changes largely agrees with the empirically inferred radiative component, both in terms of its average value and small seasonal dependence. The large uncertainties shown in Table 2, however, indeed show the need to reconcile and improve the current O_3 and H_2O data sets in terms of their long-term changes [*Hegglin et al.,* 2014].

The regression method used to separate the dynamic contribution from the radiative part (section 3) would include any radiative component that is correlated with the BDC changes in the dynamic contribution. The radiative trend in T_{LS} that is obtained based on the composition changes using the radiative calculations, however, would still contain this contribution, if any exists. Further, the BDC changes likely have an impact on the stratospheric composition (e.g., the ozone transported by the BDC trends). In order to have a consistent comparison, we quantified this effect using a regression between the monthly total radiative T_{LS} trends (black solid line in Figure 4a) and the dynamic components of T_{LS} trends over combined high latitudes (blue solid line in Figure 1a). It is thus estimated by multiplying the high latitude dynamical components by the regression coefficient for each month, which has an annual mean value of −0.01 K/decade. The total radiative trend after removing the dynamic effects associated with the BDC changes is shown in Figure 4a (black dashed line), which has an annual mean value of −0.25 K/decade. Despite the small dynamic effects, it is encouraging to see that the monthly dependence of radiative contribution after removing them (black dashed line) more closely follows the empirically derived radiative component (black solid line with x symbol in Figure 4a, i.e., red dashed line in Figure 1a). Figure 4b shows the annual mean tropical temperature trend profiles that are used to derive the corresponding annual mean T_{LS} trend values shown in Figure 4a.

6. Long-Term Change of the BDC: Tropical Residual Vertical Velocity at 70 hPa

In section 4, we showed that the T_{LS} changes attributed to those in the BDC in the last three decades were significant at a 90% confidence interval. Here we quantify the relationship between tropical residual vertical velocity (w^*) at 70 hPa and T_{LS}. We then estimate the relative change of the BDC in terms of w^* by converting the dynamic component of the tropical T_{LS} trend to the change of w^*.

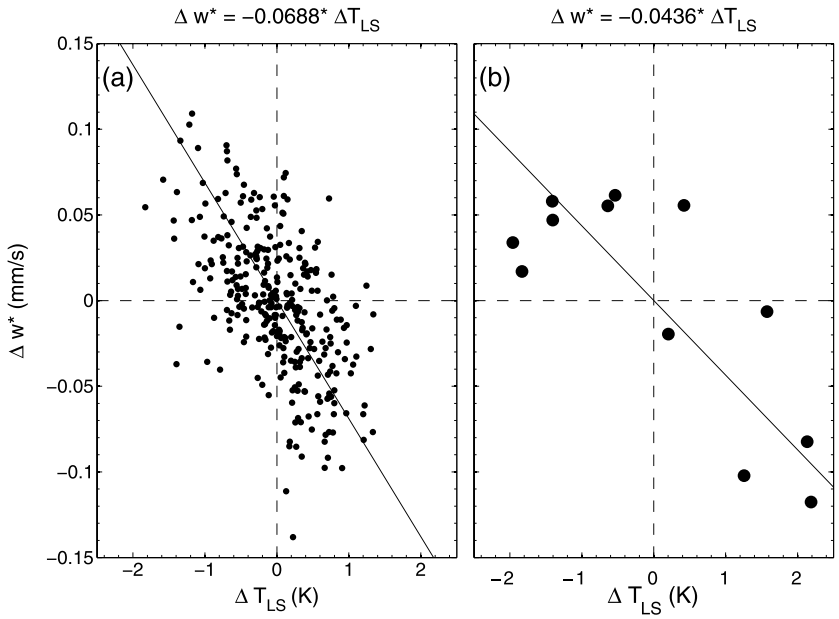

Figure 5. Tropical residual vertical velocity (w^*) (mm/s) versus T_{LS} (K) for (a) detrended monthly anomalies and (b) monthly climatology from ERA-Interim reanalysis data for the period of 1980–2009. Two years of data after the El Chichon and Pinatubo eruptions (including eruption months) are excluded.

We calculated w^* at 70 hPa from the 6-hourly ERA-Interim reanalysis data [*Lin and Fu,* 2013]. We averaged w^* over the tropics, weighted by the cosine of latitude. Its climatological mean annual cycle was determined for 1980–2009, and the monthly anomaly time series was then derived for this time period. Two years of data after the El Chichon and Pinatubo eruptions (including eruption months) were excluded. The monthly anomaly time series were detrended to avoid the impact of long-term changes. Figures 5a and 5b show w^* versus T_{LS} associated with inter-annual and seasonal variability, respectively, along with the linear fits. We obtain a relation between w^* and T_{LS} in a form of $\Delta w^* = c^* \Delta T_{LS}$, where c is −0.069 mm/s/K from the inter-annual variability and −0.044 mm/s/K from the seasonal variation. The difference in the coefficient c from the inter-annual and seasonal variations is statistically significant at the 95% confidence interval (Table 3).

The difference in the coefficients between Figures 5a and 5b could be related to the different mechanisms involved in driving the changes of vertical velocity and T_{LS} in tropical lower stratosphere. The seasonal variation of w^* and T_{LS} is the result of stronger extratropical wave activity in the winter hemisphere [*Rosenlof*, 1995]. The inter-annual variability of w^* and T_{LS} is related to the quasi-biennial oscillation [*Randel et al.,* 1999; *Yang et al.,* 2008] and the El Nino–Southern Oscillation [e.g., *Sassi et al.,* 2004; *Lin et al.,* 2012], as well as a result of the nonlinear dynamics of the atmosphere [*Garfinkel and Hartmann*, 2007]. The change of the BDC driven by extratropical wave activities could be different from that driven by tropical/subtropical waves in terms of its vertical structure [*Lin and Fu*, 2013] and thus its effect on T_{LS}. The difference in the coefficients

Table 3. The Coefficient c (mm/s/K) in $\Delta w^* = c^* \Delta T_{LS}$ From the Inter-annual and Annual Variations and Its Range in the 95% and 90% Confidence Intervals[a]

	Mean	95% Interval	90% Interval	Mean	95% Interval	90% Interval
	Inter-annual			Annual		
c (mm/s/K)	−0.069	−0.073, −0.065	−0.072, −0.066	−0.044	−0.056, −0.037	−0.054, −0.038
w^* trend (%/decade)	2.61	−0.13, 5.95	0.28, 5.34	1.68	−0.10, 3.94	0.17, 3.51

[a]The w^* relative trend (%/decade) and its range in the 95% and 90% confidence intervals for 1980–2009. The latter are derived with $\Delta w^* = c^* \Delta T_{LS}$ by considering the probability density function (pdf) of the T_{LS} dynamic component (Figure 2) and the pdf of the coefficient c, based on the Monte Carlo method. The annual mean w^* at 70 hPa over the tropics is set to be 0.288 mm/s.

could also be due to the fact that transience plays a significant role in the annual cycle but less so in inter-annual variations [*Randel et al.,* 2002]. Furthermore, the radiative damping time as well as the stability parameter [see equation (2)] depends on the atmospheric vertical structure [e.g., *Hartmann et al.,* 2001]. Although detailed mechanisms of the long-term BDC changes are still not fully understood [*SPARC CCMVal*, 2010; *Butchart*, 2014], the coefficients of −0.069 and −0.044 mm/s/K, corresponding to the BDC changes driven by extratropical and tropical wave activities, would cover a reasonable range.

Therefore, for a dynamic component of −0.11 K/decade in tropical T_{LS} trend, the corresponding change in w^* is 0.0076 and 0.0048 mm/s/decade, respectively, using the coefficients of −0.069 and −0.044 mm/s/K. The annual mean w^* at 70 hPa over the tropics is 0.288 mm/s from the ERA-Interim reanalysis. Thus, the relative strengthening of the BDC in terms of tropical residual vertical velocity at 70 hPa is estimated to be 2.6% and 1.7% per decade in the last 30 years (Table 3). By considering both the probability density function (pdf) of the T_{LS} dynamic component (Figure 2) and the pdf of the coefficient c, we can derive the pdf of w^* trend using the Monte Carlo method. Table 3 gives the range of w^* relative trend at the 95% and 90% confidence intervals using the c based on both inter-annual and seasonal variations. We see that the strengthening of the BDC is statistically significant at the 90% confidence interval. By averaging the results from the c based on inter-annual and seasonal variations, we have a w^* relative trend of ~2.1% decade^{-1} with the range of −0.1% to 5.0% decade^{-1} at 95% confidence interval and 0.2% to 4.5% decade^{-1} at 90% confidence interval.

An acceleration of the BDC in response to rising greenhouse gas concentrations and ozone depletion has been well documented in GCM and CCM simulations [e.g., *Ramaswamy et al.,* 1996; *Eichelberger and Hartmann*, 2005; *Butchart et al.,* 2006; *Li et al.,* 2008; *Garcia and Randel*, 2008; *Butchart et al.,* 2010; *Lin and Fu*, 2013]. In order to have a direct comparison of simulated BDC changes with our observational analysis, we used the residual vertical velocity w^* at 70 hPa archived in the CCMVal-2 database. The monthly anomaly time series of w^* at 70 hPa, averaged over the tropics, from 1980 to 2004 were derived for the 11 CCMs. The mean relative increase of tropical w^* at 70 hPa is 1.9% per decade, ranging from −0.1% to 6%, for the 11 CCMs, which agrees well with our observational results (see Table 3).

7. Summary and Conclusions

The change of the BDC during the period of 1980–2009 was examined through a combined analysis of satellite MSU/AMSU T_{LS}, observed evolutions of well-mixed greenhouse gases, O_3, H_2O, as well as stratospheric aerosols, and reanalysis data. The MSU/AMSU-observed tropical T_{LS} trend is first empirically separated into a dynamic component associated with the BDC changes and a radiative component due to the atmospheric composition changes. A statistical analysis of these derived trends was performed, with uncertainties based on a Monte Carlo technique. The data suggest that the annual mean BDC has accelerated in the last 30 years with 90% confidence and that the acceleration of the SH annual mean BDC cell is statistically significant, while the changes are not significant in the NH. The insignificant long-term change of the NH BDC cell implies that we should expect an insignificant long-term change of mean age of stratospheric air in the NH.

The radiative component of tropical T_{LS} trends was also examined based on observed changes in stratospheric composition. The changes in O_3, stratospheric aerosols, well-mixed greenhouse gases, and H_2O all make significant contributions to the radiative component of tropical T_{LS} trends for 1980–2009. Despite large uncertainties in lower stratospheric cooling associated with uncertainties in the observed O_3 and H_2O changes there, the derived radiative component agrees with the empirically inferred value and supports the view that the radiative component of tropical T_{LS} trends has small seasonal dependence.

We have further established an empirical relationship between tropical residual vertical velocity at 70 hPa and T_{LS} so that the dynamic component of tropical T_{LS} trends can be used to estimate the change in tropical residual vertical velocity. The relative acceleration of the annual mean BDC in terms of tropical residual vertical velocity at 70 hPa was estimated to be ~2.1% decade^{-1} with the range of −0.1% to 5.0% decade^{-1} at 95% confidence interval and 0.2% to 4.5% decade^{-1} at 90% confidence interval, for 1980–2009 on this basis. The relative acceleration of the annual mean BDC from 11 CCMs gives a mean value of 1.9% per decade, ranging from −0.1% to 6% per decade, which agrees well with our observational analysis.

Acknowledgments
We gratefully acknowledge the modeling groups for making their simulations available for this analysis, the Chemistry-Climate Model Validation (CCMVal) Activity for WCRP's (World Climate Research Programme) SPARC (Stratospheric Processes and their Role in Climate) project for organizing and coordinating the model data analysis activity, and the British Atmospheric Data Center (BADC) for collecting and archiving the CCMVal model output. This research was supported by NASA grants NNX13AN49G and NNX14AB28G, and the Office of Science (BER), U.S. Department of Energy: grant DE-SC0010557. S.S. was partly supported by NSF grants 1342810 and 1461517. Contact Qiang Fu (qfuatm@gmail.com) for the data used in this paper.

References

Andrews, D. G., J. R. Holton, and C. B. Leovy (1987), *Middle Atmosphere Dynamics*, *Intl. Geophys. Ser.*, vol. 40, 489 pp., Academic Press, San Diego, Calif.
Birner, T. (2010), Residual circulation and tropopause structure, *J. Atmos. Sci.*, *67*, 2582–2600.
Butchart, N. (2014), The Brewer-Dobson circulation, *Rev. Geophys.*, *52*, 157–184, doi:10.1002/2013RG000448.
Butchart, N., et al. (2006), Simulations of anthropogenic change in the strength of the Brewer-Dobson circulation, *Clim. Dyn.*, *27*, 727–741, doi:10.1007/s00382-006-0162-4.
Butchart, N., et al. (2010), Chemistry-climate model simulations of twenty first century stratospheric climate and circulation changes, *J. Clim.*, *23*, 5349–5374, doi:10.1175/2010JCLI3404.1.
Christy, J. R., R. W. Spencer, W. B. Norris, W. D. Braswell, and D. E. Parker (2003), Error estimates of version 5.0 of MSU-AMSU bulk atmospheric temperatures, *J. Atmos. Oceanic Technol.*, *20*, 613–629.
Cionni, L., V. Eyring, J. F. Lamarque, W. J. Randel, D. S. Stevenson, F. Wu, G. E. Bodeker, T. G. Shepherd, D. T. Shindell, and D. W. Waugh (2011), Ozone database in support of CMIP5 simulations: Results and corresponding radiative forcing, *Atmos. Chem. Phys.*, *11*, 11,267–11,292, doi:10.5194/acp-11-11267-2011.
Dee, D. P., et al. (2011), The ERA-Interim reanalysis: Configuration and performance of the data assimilation system, *Q. J. R. Meteorol. Soc.*, *137*, 553–597, doi:10.1002/qj.828.
Dessler, A. E., M. R. Schoeberl, T. Wang, S. M. Davis, and K. H. Rosenlof (2013), Stratospheric water vapor feedback, *Proc. Natl. Acad. Sci. U.S.A.*, *110*, 18,087–18,091.
Eichelberger, S. J., and D. L. Hartmann (2005), Changes in the strength of the Brewer-Dobson circulation in a simple AGCM, *Geophys. Res. Lett.*, *32*, L15807, doi:10.1029/2005GL022924.
Engel, A., et al. (2009), Age of stratospheric air unchanged within uncertainties over the past 30 years, *Nat. Geosci.*, *2*, 28–31.
Eyring, V., et al. (2007), Multimodel projections of stratospheric ozone in the 21st century, *J. Geophys. Res.*, *112*, D16303, doi:10.1029/2006JD008332.
Forster, P. M. F., and K. P. Shine (1997), Radiative forcing ad temperature trends from stratospheric ozone changes, *J. Geophys. Res.*, *102*, 10,841–10,855, doi:10.1029/96JD03510.
Free, M. (2011), The seasonal structure of temperature trends in the tropical lower stratosphere, *J. Clim.*, *24*, 859–866.
Fu, Q. (2013), Bottom up in the tropics, *Nat. Clim. Change*, *3*, 957–958.
Fu, Q., and C. M. Johanson (2005), Satellite-derived vertical dependence of tropical tropospheric temperature trends, *Geophys. Res. Lett.*, *32*, L10703, doi:10.1029/2004GL022266.
Fu, Q., and K. N. Liou (1992), On the correlated k-distribution method for radiative transfer in nonhomogeneous atmosphere, *J. Atmos. Sci.*, *49*, 2139–2156.
Fu, Q., C. M. Johanson, S. G. Warren, and D. J. Seidel (2004), Contribution of stratospheric cooling to satellite-inferred tropospheric temperature trends, *Nature*, *429*, 55–58.
Fu, Q., S. Solomon, and P. Lin (2010), On the seasonal dependence of tropical lower-stratospheric temperature trends, *Atmos. Chem. Phys.*, *10*, 2643–2653.
Fu, Q., S. Manabe, and C. M. Johanson (2011), On the warming in the tropical upper troposphere: Models versus observations, *Geophys. Res. Lett.*, *38*, L15704, doi:10.1029/2011GL048101.
Fueglistaler, S., and P. H. Haynes (2005), Control of interannual and longer-term variability of stratospheric water vapor, *J. Geophys. Res.*, *110*, D24108, doi:10.1029/2005JD006019.
Fueglistaler, S., A. E. Dessler, T. J. Dunkerton, I. Folkins, Q. Fu, and P. W. Mote (2009), Tropical tropopause layer, *Rev. Geophys.*, *47*, RG1004, doi:10.1029/2008RG000267.
Fueglistaler, S., P. H. Haynes, and P. M. Forster (2011), The annual cycle in lower stratospheric temperatures revisited, *Atmos. Chem. Phys.*, *11*, 3701–3711.
Garcia, R. R., and W. J. Randel (2008), Acceleration of the Brewer-Dobson circulation due to increases in greenhouse gases, *J. Atmos. Sci.*, *65*, 2731–2739.
Garcia, R. R., W. J. Randel, and D. E. Kinnison (2011), On the determination of age of air trends from atmospheric trace species, *J. Atmos. Sci.*, *68*, 139–154.
Garfinkel, C. I., and D. L. Hartmann (2007), Effects of the El Nino-Southern Oscillation and the quasi-biennial oscillation on polar temperatures in the stratosphere, *J. Geophys. Res.*, *112*, D19112, doi:10.1029/2007JD008481.
Hartmann, D. L., J. R. Holton, and Q. Fu (2001), The heat balance of the tropical tropopause, cirrus, and stratospheric dehydration, *Geophys. Res. Lett.*, *28*(10), 1969–1972, doi:10.1029/2000GL012833.
Hassler, B., G. Bodeker, I. Cionni, and M. Dameris (2009), A vertically resolved, monthly mean, ozone database from 1979 to 2100 for constraining global climate model simulations, *Int. J. Remote Sens.*, *30*, 4009–4018, doi:10.1080/01431160902821874.
Hegglin, M. I., et al. (2014), Vertical structure of stratospheric water vapour trends derived from merged satellite data, *Nat. Geosci.*, *7*, 768–776.
Holton, J. R., P. H. Haynes, M. E. McIntyre, A. R. Douglass, R. B. Rood, and L. Pfister (1995), Stratosphere-troposphere exchange, *Rev. Geophys.*, *33*, 403–439, doi:10.1029/95RG02097.
Hu, Y., and Q. Fu (2009), Stratospheric warming in Southern Hemisphere high latitudes since 1979, *Atmos. Chem. Phys.*, *9*, 4329–4340.
Johanson, C. M., and Q. Fu (2007), Antarctic atmospheric temperature trend patterns from satellite observations, *Geophys. Res. Lett.*, *34*, L12703, doi:10.1029/2006GL029108.
Lamarque, J.-F., and S. Solomon (2010), Impact of changes in climate and halocarbons on recent lower stratosphere ozone and temperature trends, *J. Clim.*, *23*, 2599–2611, doi:10.1175/2010JCLI3179.1.
Li, F., J. Austin, and J. Wilson (2008), The strength of the Brewer-Dobson circulation in a changing climate: Coupled chemistry-climate model simulations, *J. Clim.*, *21*, 40–57, doi:10.1175/2007JCLI1663.1.
Li, F., R. S. Stolarski, and P. A. Newman (2009), Stratospheric ozone in the post-CFC era, *Atmos. Chem. Phys.*, *6*, 2207–2213.
Lin, P., and Q. Fu (2013), Changes in various branches of the Brewer-Dobson circulation from an ensemble of chemistry climate models, *J. Geophys. Res. Atmos.*, *118*, 73–84, doi:10.1029/2012JD018813.
Lin, P., Q. Fu, S. Solomon, and J. M. Wallace (2009), Temperature trend patterns in Southern Hemisphere high latitudes: Novel indicators of stratospheric change, *J. Clim.*, *22*, 6325–6341, doi:10.1175/2009JCLI2971.1.
Lin, P., Q. Fu, and D. L. Hartmann (2012), Impact of tropical SST on stratospheric planetary waves in the Southern Hemisphere, *J. Clim.*, *25*, 5030–5046.
Manzini, E., et al. (2014), Northern winter climate change: Assessment of uncertainty in CMIP5 projections related to stratosphere-troposphere coupling, *J. Geophys. Res. Atmos.*, *119*, 7979–7998, doi:10.1002/2013JD021403.

Mears, C. A., and F. J. Wentz (2009), Construction of the Remote Sensing Systems V3.2 atmospheric temperature records from the MSU and AMSU microwave sounders, *J. Atmos. Oceanic Technol.*, *26*, 1040–1056.
Mlawer, E. J., and S. A. Clough (1998), Shortwave and longwave enhancements in the rapid radiative transfer model, *Proceedings of the 7th Atmospheric Radiation Measurement (ARM) Science Team Meeting*, U.S. Dep. of Energy, CONF-970365.
Mlawer, E. J., S. J. Taubman, P. D. Brown, M. J. Iacono, and S. A. Clough (1997), RRTM, a validated correlated-k model for the longwave, *J. Geophys. Res.*, *102*, 16,663–16,682, doi:10.1029/97JD00237.
Newman, P. A., E. R. Nash, and J. E. Rosenfield (2001), What controls the temperature of the Arctic stratosphere during the spring?, *J. Geophys. Res.*, *106*(D17), 19,999–20,010, doi:10.1029/2000JD000061.
Oltmans, S. J., H. Vo¨mel, D. J. Hofmann, K. H. Rosenlof, and D. Kley (2000), The increase in stratospheric water vapor from ballonborne, frostpoint hygrometer measurements at Washington, D.C., and Boulder, Colorado, *Geophys. Res. Lett.*, *27*, 3453–3456, doi:10.1029/2000GL012133.
Oman, L., D. W. Waugh, S. Pawson, R. S. Stolarski, and P. A. Newman (2009), On the influence of anthropogenic forcings on changes in the stratospheric mean age, *J. Geophys. Res.*, *114*, D03105, doi:10.1029/2008JD010378.
Osso, A., Y. Sola, K. Rosenlof, B. Hassler, J. Bech, and J. Lorente (2015), How robust are trends in the Brewer–Dobson circulation derived from observed stratospheric temperatures?, *J. Clim.*, *28*, 3024–3040.
Plumb, R. A. (2002), Stratospheric transport, *J. Met. Soc. Japan*, *80*, 793–809.
Po-Chedley, S., and Q. Fu (2012), Discrepancies in tropical upper tropospheric warming between atmospheric circulation models and satellites, *Environ. Res. Lett.*, *7*(8pp), 044,018, doi:10.1088/1748-9326/7/4/044018.
Ramaswamy, V., M. D. Schwarzkopf, and W. J. Randel (1996), Fingerprint of ozone depletion in the spatial and temporal pattern of recent lower-stratospheric cooling, *Nature*, *382*, 616–618.
Randel, W. J., and A. M. Thompson (2011), Interannual variability and trends in tropical ozone derived from SAGE II satellite data and SHADOZ ozonesondes, *J. Geophys. Res.*, *116*, D07303, doi:10.1029/2010JD015195.
Randel, W. J., and F. Wu (2007), A stratospheric ozone profile data set for 1979–2005: Variability, trends, and comparisons with column ozone data, *J. Geophys. Res.*, *112*, D06313, doi:10.1029/2006JD007339.
Randel, W. J., F. Wu, R. Swinbank, J. Nash, and A. O'Neil (1999), Global QBO circulation derived from UKMO stratospheric analyses, *J. Atmos. Sci.*, *56*, 457–474.
Randel, W. J., R. R. Garcia, and F. Wu (2002), Time-dependent upwelling in the tropical lower stratosphere estimated from the zonal-mean momentum budget, *J. Atmos. Sci.*, *59*, 2141–2152.
Randel, W. J., F. Wu, H. Vo¨mel, G. E. Nedoluha, and P. Forster (2006), Decreases in stratospheric water vapor after 2001: Links to changes in the tropical tropopause and the Brewer-Dobson circulation, *J. Geophys. Res.*, *111*, D12312, doi:10.1029/2005JD006744.
Rose, F. G., and T. P. Charlock (2002), New Fu-Liou code tested with ARM Ramen lidar and CERES in pre-CALIPSO exercise, *Proceedings of the 11th Conference on Atmospheric Radiation*, Ogden, Utah, 3–7 June.
Rosenlof, K. H. (1995), Seasonal cycle of the residual mean meridional circulation in the stratosphere, *J. Geophys. Res.*, *100*, 5173–5191, doi:10.1029/94JD03122.
Rosenlof, K. H., and G. C. Reid (2008), Trends in the temperature and water vapor content of the tropical lower stratosphere: Sea surface connection, *J. Geophys. Res.*, *113*, D06107, doi:10.1029/2007JD009109.
Russell, J. M., III, A. F. Tuck, L. L. Gordley, J. H. Park, S. R. Drayson, J. E. Harries, R. J. Cicerone, and P. J. Crutzen (1993), The Halogen Occultation Experiment, *J. Geophys. Res.*, *98*, 10,777–10,797, doi:10.1029/93JD00799.
Sassi, F., D. Kinneson, B. A. Boville, R. R. Garcia, and R. Roble (2004), Effect of El Nino–Southern Oscillation on the dynamical, thermal, and chemical structure of the middle atmosphere, *J. Geophys. Res.*, *109*, D17108, doi:10.1029/2003JD004434.
Sato, M., J. E. Hansen, M. P. McCormick, and J. B. Pollack (1993), Stratospheric aerosol optical depth, 1850–1990, *J. Geophys. Res.*, *98*, 22,987–22,994, doi:10.1029/93JD02553.
Seviour, W. J. M., N. Butchart, and S. C. Hardiman (2012), The Brewer-Dobson circulation inferred from ERA-Interim, *Q. J. Roy. Meteorol. Soc.*, *138*, 878–888, doi:10.1002/qj.966.
Shepherd, T. G. (2008), Dynamics, stratospheric ozone, and climate change, *Atmos.-Ocean*, *46*, 117–138.
Shepherd, T. G., and C. McLandress (2011), A robust mechanism for strengthening of the Brewer-Dobson circulation in response to climate change: Critical-layer control of subtropical wave breaking, *J. Atmos. Sci.*, *68*, 784–797, doi:10.1175/2010JAS3608.1.
Sioris, C. E., C. A. McLinden, V. E. Fioletov, C. Adams, J. M. Zawodny, A. E. Bourassa, C. Z. Roth, and D. A. Degenstein (2014), Trend and variability in ozone in the tropical lower stratosphere over 2.5 solar cycles observed by SAGE II and OSIRIS, *Atmos. Chem. Phys.*, *14*, 3479–3496.
Solomon, S., K. H. Rosenlof, R. W. Portmann, J. S. Daniel, S. M. Davis, T. J. Sanford, and G.-K. Plattner (2010), Contributions of stratospheric water vapor to decadal changes in the rate of global warming, *Science*, *327*, 1219–1223.
Solomon, S., J. S. Daniel, R. R. Neely III, J.-P. Vernier, E. G. Dutton, and L. W. Thomason (2011), The persistently variable "background" stratospheric aerosol layer and global climate change, *Science*, *333*, 866–870.
Solomon, S., P. J. Young, and B. Hassler (2012), Uncertainties in the evolution of stratospheric ozone and implications for recent temperature changes in the tropical lower stratosphere, *Geophys. Res. Lett.*, *39*, L17706, doi:10.1029/2012GL052723.
SPARC CCMVal (2010), Chemistry-climate model validation, *SPARC Rep. 5, WCRP-30, WMO/TD-40*. [Available at http://www.sparc-climate.org/publications/sparc-reports/sparc-report-no5/.]
Taylor, K. E., R. J. Stouffer, and G. A. Meehl (2012), An overview of CMIP5 and the experiment design, *Bull. Am. Meteorol. Soc.*, *93*, 485–498.
Thompson, A. M., et al. (2003), Southern Hemisphere Additional Ozonesondes (SHADOZ) 1998–2000 tropical ozone climatology: 1. Comparison with Total Ozone Mapping Spectrometer (TOMS) and ground-based measurements, *J. Geophys. Res.*, *108*(D2), 8238, doi:10.1029/2001JD000967.
Thompson, D. W. J., and S. Solomon (2005), Recent stratospheric climate trends as evidenced in radiosonde data: Global structure and tropospheric linkages, *J. Clim.*, *18*, 4785–4795.
Thompson, D. W. J., and S. Solomon (2009), Understanding recent stratospheric climate change, *J. Clim.*, *22*, 1934–1943.
Vernier, J. P., et al. (2011), Major influence of tropical volcanic eruptions on the stratospheric aerosol layer during the last decade, *Geophys. Res. Lett.*, *38*, L12807, doi:10.1029/2011GL047563.
Waugh, D. W. (2009), The age of stratospheric air, *Nat. Geosci.*, *2*, 14–16.
WMO (2011), Scientific assessment of ozone depletion: 2010, Global Ozone Research and Monitoring Project-Report 52, Geneva, Switzerland.
Yang, Q., Q. Fu, J. Austin, A. Gettelman, F. Li, and H. Vomel (2008), Observationally derived and general circulation model simulated tropical stratospheric upward mass fluxes, *J. Geophys. Res.*, *113*, D00B07, doi:10.1029/2008JD009945.
Young, P. J., K. H. Rosenlof, S. Solomon, S. C. Sherwood, Q. Fu, and J.-F. Lamarque (2012), Changes in stratospheric temperatures and their implications for changes in the Brewer-Dobson circulation, 1979–2005, *J. Clim.*, *25*, 759–1772, doi:10.1175/2011JCLI4048.1.

Yulaeva, E., J. R. Holton, and J. M. Wallace (1994), On the cause of the annual cycle in tropical lower-stratospheric temperatures, *J. Atmos. Sci.*, *51*, 169–174.

Zhao, M., I. M. Held, S. J. Lin, and G. A. Vecchi (2009), Simulations of global hurricane climatology, interannual variability, and response to global warming using a 50-km resolution GCM, *J. Clim.*, *22*, 6653–6678.

Zou, C. Z., M. D. Goldberg, Z. Cheng, N. C. Grody, J. T. Sullivan, C. Cao, and D. Tarpley (2006), Recalibration of microwave sounding unit for climate studies using simultaneous nadir overpasses, *J. Geophys. Res.*, *111*, D19114, doi:10.1029/2005JD006798.